Orbital polarons versus itinerant e_g electrons in doped manganites

Maria Daghofer,[1] Andrzej M. Oleś,[2] and Wolfgang von der Linden[1]
[1]*Institute of Theoretical and Computational Physics, Graz University of Technology, Petersgasse 16, A-8010 Graz, Austria*
[2]*Marian Smoluchowski Institute of Physics, Jagellonian University, Reymonta 4, PL-30059 Kraków, Poland*
(Received 31 May 2004; published 23 November 2004)

We study an effective one-dimensional (1-D) orbital *t-J* model derived for strongly correlated e_g electrons in doped manganites. The ferromagnetic spin order at half filling is supported by orbital superexchange $\propto J$ which stabilizes orbital order with alternating x^2-y^2 and $3z^2-r^2$ orbitals. In a doped system it competes with the kinetic energy $\propto t$. When a single hole is doped to a half-filled chain, its motion is hindered and a localized *orbital polaron* is formed. An increasing doping generates either separated polarons or phase separation into hole-rich and hole-poor regions, and eventually polarizes the orbitals and gives a *metallic phase* with occupied $3z^2-r^2$ orbitals. This crossover, investigated by exact diagonalization at zero temperature, is demonstrated both by the behavior of correlation functions and by spectral properties, showing that the orbital chain with Ising superexchange is more classical and thus radically different from the 1-D spin *t-J* model. At finite temperature we derive and investigate an effective 1-D orbital model using a combination of exact diagonalization with classical Monte Carlo for spin correlations. A competition between the antiferromagnetic and ferromagnetic spin order was established at half filling, and localized polarons were found for antiferromagnetic interactions at low hole doping. Finally, we clarify that the Jahn-Teller alternating potential stabilizes the orbital order with staggered orbitals, inducing the ferromagnetic spin order, and enhancing the localized features in the excitation spectra. Implications of these findings for colossal magnetoresistance manganites are discussed.

DOI: 10.1103/PhysRevB.70.184430 PACS number(s): 75.47.Lx, 75.10.Lp, 71.30.+h, 79.60.-i

I. INTRODUCTION

Doped perovskite manganese oxides $R_{1-x}A_xMnO_3$, where R and A are rare earth and alkaline earth ions, have attracted increasing attention because they show a rich variety of electronic, magnetic, and structural phenomena, and several different types of ordered phases.[1] To explain the colossal magnetoresistence[2] (CMR) and metal-insulator transition observed in these compounds as a function of either doping x or temperature T, which suggests their potential technological applications, one has to go beyond the simple double exchange model of Zener,[3] and investigate a complex interplay between magnetic, orbital, and lattice degrees of freedom, as well as the conditions for the itinerant behavior of strongly correlated e_g electrons.

The theoretical challenge is to understand the properties of doped manganites in terms of the dynamics of correlated e_g electrons which involves their orbital degrees of freedom.[1,4] Although several features such as the transition to ferromagnetic (FM) order under doping, and the magnetic excitations in the FM phase, were qualitatively reproduced within the Kondo model which assumes a nondegenerate conduction band,[1,5–11] it is evident that the degeneracy of e_g orbitals plays a major role in the double exchange model, in the transport properties of doped manganites, and in the CMR effect itself.[12–14] In the undoped $LaMnO_3$ charge fluctuations are suppressed by large on-site Coulomb interaction U, leading to superexchange which involves both spin and orbital e_g degrees of freedom.

Purely electronic superexchange models describing the orbital order of e_g electrons were suggested early on by Kugel and Khomskii,[15] and are of great interest recently.[16] In cuprates, like in $KCuF_3$, they lead to enhanced quantum effects,[17] while in manganites these models, which originate from several charge excitations due to either e_g or t_{2g} electrons, are richer and include interactions between large and more classical spins.[18–21] These interactions, together with the Jahn-Teller (JT) effect, stabilize *A*-type antiferromagnetic (AF) phase coexisting with orbital order in undoped $LaMnO_3$. While the shape of the occupied orbitals in the low-temperature phase of $LaMnO_3$ is still controversial, the two-sublattice orbital alternation in an orbital ordered state within the FM planes of $LaMnO_3$ is well established.[22] When the spin dynamics in the FM planes of $LaMnO_3$ is frozen at low temperature, one can constrain an effective model to *purely orbital superexchange*[23] instead of considering a more complex complete spin-orbital model.[20] The superexchange orbital interactions favor then alternating directional ($3z^2-r^2$-like) and planar (x^2-y^2-like) orbitals along every cubic direction.[23]

A considerable simplification is allowed in the FM phase at finite doping and at $T=0$, where the spins are aligned and an effective *t-J*-like charge-orbital model is sufficient. Experimentally, at doping higher than $x\simeq 0.10$ one finds a FM insulating phase, followed by a metallic phase.[24] The microscopic reasons of this behavior are intriguing—it contradicts the usual spin polaronic picture of a FM phase. A puzzling competition between the insulating and metallic behavior within the FM phase was also reported for $La_{0.88}Sr_{0.12}MnO_3$.[25]

Here we will concentrate on the generic behavior due to e_g *orbital degrees of freedom* in a FM phase, and we will treat the spin dynamics classically, as usually done in the double exchange model.[3,13] This approach is complementary to focusing on the quantum effects in double exchange, which was presented recently.[26] Our aim is to study the correlation functions and spectral properties of a one-dimensional (1-D) orbital *t-J* model by exact diagonalization at zero temperature ($T=0$), and by classical Monte Carlo simulations of spin correlations at finite temperature in order

to establish the consequences of orbital order and orbital dynamics in doped manganites. In the strongly correlated regime the charge dynamics couples to orbital excitations and can be described in terms of the orbital *t*-*J* model for doped manganites.[14,27,28] As in the spin *t*-*J* model, a doped hole moves in an orbital ordered state by dressing itself with orbital excitations.[27] However, the structure of the quasiparticle (orbital polaron[28]) is here quite different from that derived from the *t*-*J* model,[29] as the orbital model is more classical.

As a reference system we use a 1-D spin *t*-*J* model for which the behavior of a single hole is well understood. A hole created in a 1-D Néel state is here mobile and may be thought of as decaying into a magnetic domain wall. In fact, it gives a charged domain wall already after a single hop and leaves behind a solitonic defect from which it separates and next propagates independently. This is the simplest visualization of hole-spin separation in a 1-D system. The familar string picture and quasiparticles on the energy scale of $\sim 2J$ are then recovered when a staggered magnetic field is applied and suppresses domains of reversed spins.[30,31]

We show below that an analogous phenomenon of hole-orbital separation does not occur for the orbital degrees of freedom, but instead a single hole is trapped in a 1-D chain when orbitals alternate. This explains why an insulating behavior may extend to finite doping. A staggered field has a well established physical origin in this case, and could follow from the frozen JT modes with alternating oxygen distortions along the chain itself, and on the bonds perpendicular to its direction, when the chain is embedded within a three-dimensional (3-D) crystal. This interaction may also play an important role for the transport properties of lightly doped manganites and is difficult to separate from on-site Coulomb interaction U.[32] Therefore, it was even suggested that models including Hund's exchange J_H between conductions electrons and t_{2g} spins, but neglecting Coulomb interaction U, could capture the essential physics of manganites.[33] We will investigate below the JT term which leads to a staggered field acting on the orbitals. Note, however, that the 1-D case is special as static JT distortions, preventing fluctuations of occupied orbitals, suppress completely hole motion along the chain, while in a two-dimensional (2-D) model they lead instead to an enhanced coherent component in the hole motion mainly due to the suppression of incoherent processes.[28]

Another feature characteristic of the orbital physics and different from spin models is that the lattice responds to the doping. As pointed out by Kilian and Khaliullin,[34] the breathing motion of the MnO_6 octahedra provides a strong tendency towards hole localization in the presence of singly occupied (almost) degenerate e_g levels, as shown in a 2-D model.[28] A static hole polarizes then the orbitals occupied by e_g electrons in its neighborhood, and this polarization is expected to happen in addition to the effects promoted by the orbital superexchange interactions. We also consider this interaction in the present 1-D model and show that it simply renormalizes the superexchange interaction, and thus it could lead to qualitatively new features and be of more importance only in a higher dimension.

The paper is organized as follows. In Sec. II we present the effective *t*-*J* orbital model for e_g electrons moving along a 1-D chain in a FM plane of, e.g., $La_{1-x}Sr_xMnO_3$. In Sec. III this model is analyzed first qualitatively by comparing the energies of two phases: (i) the insulating phase with localized e_g polarons, and (ii) the metallic phase with itinerant carriers. Next we analyze the correlation functions and the spectral properties of a finite chain of $N=14$ sites filled by up to five holes, and demonstrate a crossover from the insulating to metallic phase under increasing doping. At finite temperature T we derive an effective orbital *t*-*J* model, with electron hopping and orbital interactions depending on the actual configuration of core spins (Sec. IV). The interrelation between spin and orbital order, the correlations around a doped hole, and the evolution of spectral properties under increasing doping are next investigated using a combination of exact diagonalization with Monte Carlo simulations. Finally, we summarize the results and present general conclusions in Sec. V.

II. ORBITAL *t*-*J* MODEL

We consider the 1-D orbital *t*-*J* model,

$$\mathcal{H}_0 = H_t + H_J + H_{\rm JT}, \tag{1}$$

obtained for e_g electrons in FM manganites at $T=0$. The Hamiltonian (1) acts in the restricted Hilbert space without double occupancies. Due to the absence of the SU(2) symmetry, the kinetic energy in the e_g band takes a form which depends on the used orbital basis. For the present 1-D model it is most convenient to consider a chain along the c axis and to use the usual orbital basis $\{x^2-y^2, 3z^2-r^2\}$, for which we introduce a compact notation,

$$|x\rangle \equiv \frac{1}{\sqrt{2}}|x^2-y^2\rangle,\ |z\rangle \equiv \frac{1}{\sqrt{6}}|3z^2-r^2\rangle. \tag{2}$$

A chain along the a or b axis could also be analyzed using this basis,[33] but in each case one obtains a simpler and more transparent interpretation of the results with a basis consisting of a directional orbital along this particular cubic axis, and an orthogonal to it planar orbital, e.g., $3x^2-r^2$ and y^2-z^2 for an a axis.

The model given by Eq. (1) stands for a chain composed of Mn^{3+} and Mn^{4+} ions coupled by the effective hopping t, which originates from the transitions over oxygens. Due to the symmetry, the $|x\rangle$ electrons cannot move, and the hopping term H_t allows only for intersite transitions between a site occupied by a $|z\rangle$ electron and an empty neighboring site,

$$H_t = -t\sum_i (\tilde{c}^\dagger_{iz}\tilde{c}_{i+1,z} + \tilde{c}^\dagger_{i+1,z}\tilde{c}_{iz}), \tag{3}$$

where an operator $\tilde{c}^\dagger_{iz}=c^\dagger_{iz}(1-n_{ix})$ creates a $|z\rangle$ electron when site i is unoccupied by an $|x\rangle$ electron. The hopping H_t describes thus spinless fermions with an orbital flavor in a restricted Hilbert space, in analogy to the original *t*-*J* model in spin space,[35] but only one (z) component is here *itinerant*, while the other (x) one is *immobile* and hinders the motion of $|z\rangle$ electrons along the chain.

The superexchange in undoped $LaMnO_3$ is given by a superposition of several terms which originate from charge excitations due to either e_g or t_{2g} electron hopping[20]—they

are discussed in Sec. IV A. While the t_{2g} part is AF, the e_g terms favor either FM or AF spin order on a bond $\langle ij\rangle$, depending on the pair of occupied e_g orbitals at sites i and j. For the realistic parameters of $LaMnO_3$, one finds the A-type AF order in the ground state, with FM planes staggered along the third direction. Taking a cubic c direction within a FM plane, the superexchange expression simplifies enormously.[23] Treating large $S=2$ spins at Mn^{3+} ions classically, all AF terms drop out at $T=0$, and the remaining *orbital superexchange* favors alternating e_g orbitals.[36] Therefore, the superexchange interactions reduce then to the purely orbital interactions which favor alternating directional ($3z^2-r^2$-like) and planar (x^2-y^2-like) orbitals along every cubic direction.[23] In the present 1-D model one finds

$$H_J = 2J\sum_i \left(T_i^z T_{i+1}^z - \tfrac{1}{4}\tilde{n}_i\tilde{n}_{i+1}\right), \tag{4}$$

where operators

$$T_i^z = \tfrac{1}{2}\sigma_i^z = \tfrac{1}{2}(n_{ix} - n_{iz}), \tag{5}$$

stand for orbital pseudospins $T=1/2$, with two eigenstates defined in Eq. (2), and $\tilde{n}_i = \tilde{c}_{ix}^\dagger \tilde{c}_{ix} + \tilde{c}_{iz}^\dagger \tilde{c}_{iz}$ is an electron number operator in the restricted Hilbert space. The superexchange constant $J=t^2/\varepsilon(^6A_1)$ is then given by the high-spin excitation energy $\varepsilon(^6A_1)$.[20]

The last term in Eq. (1) stands for the staggered field induced by the cooperative JT effect,

$$H_{\rm JT} = 2E_{\rm JT}\sum_i \exp(i\pi R_i) T_i^z, \tag{6}$$

considered also in Ref. 37, and supporting the alternating orbital order. It gives an energy gain $E_{\rm JT}$ per site in the ground state of an undoped 1-D chain, and follows from the alternating oxygen distortions around manganese ions in $LaMnO_3$.[38] The present simplified form [Eq. (6)] of a general expression,[39] which depends on the type of oxygen distortion, is sufficient in the 1-D model.

At finite doping $x=1-n$, where n is an average e_g electron number per site, the present t-J model gives an interesting problem, with competing tendencies towards orbital alternation in insulating state on one hand, described by orbital correlations,

$$T(n) = \langle T_i^z T_{i+n}^z\rangle, \tag{7}$$

and uniform $|z\rangle$ polarization in the metallic state on the other. The nature of the ground state obtained at finite doping is best investigated by considering a few characteristic correlation functions, containing information about the orbital state and about the orbital order between two nearest neighbor sites, both at distance n from a hole and about the orbital correlations across a hole. To optimize them we introduce

$$P(n) = \langle \overline{n_i} T_{i+n}^z\rangle, \tag{8}$$

$$R(n) = \langle \overline{n_i} T_{i+n}^z T_{i+n+1}^z\rangle, \tag{9}$$

$$Z = \langle T_{i-1}^z \overline{n_i} T_{i+1}^z\rangle, \tag{10}$$

where $\overline{n_i}$ is a hole number operator at site i,

$$\overline{n_i} = 1 - \tilde{c}_{iz}^\dagger \tilde{c}_{iz} - \tilde{c}_{ix}^\dagger \tilde{c}_{ix}. \tag{11}$$

These correlation functions will be discussed in Secs. III and IV. Note that the kinematical constraint gives $P(0)=R(0)=0$.

We compare the orbital correlations and the spectral properties obtained for the orbital chain, with these found for a 1-D t-J spin model for $S=1/2$ spins,

$$\mathcal{H}_{tJ} = -t\sum_{i\sigma}(\tilde{c}_{i\sigma}^\dagger \tilde{c}_{i+1,\sigma} + \tilde{c}_{i+1,\sigma}^\dagger \tilde{c}_{i\sigma}) + 2J\sum_i \left(\vec{S}_i\cdot\vec{S}_{i+1} - \tfrac{1}{4}\tilde{n}_i\tilde{n}_{i+1}\right) + 2h_s\sum_i \exp(i\pi R_i) S_i^z, \tag{12}$$

where $\tilde{c}_{i\sigma}^\dagger = c_{i\sigma}^\dagger(1-n_{i,-\sigma})$ is a creation operator of an electron with spin σ at site i in the restricted Hilbert space. In contrast to the orbital model, here the electrons with *both spin flavors are mobile* and exchange between the sites i and $i+1$, so the interaction is a scalar product $\vec{S}_i\cdot\vec{S}_{i+1}$ instead of the Ising term $T_i^z T_{i+1}^z$. For convenience, we use the same units as in Eqs. (4) and (6); here $J=2t^2/U$ with U being the excitation energy. The staggered field $\propto h_s$ simulates the long-range spin order present in a 2-D model,[30,31] and plays a similar role to the JT field in the present orbital model. For doped spin chain we consider analogous correlation functions to orbital-orbital (7), hole-orbital (8), orbital order at distance n from the hole (9), and around a hole (10), with spin operators S_i^z in place of T_i^z [Eq. (5)].

In the next section we report the results obtained by Lanczos diagonalization of an $N=14$ orbital chain with periodic boundary conditions and different electron filling at $T=0$, and compare them to more familiar spin physics. We have verified that the results concerning the crossover to a metallic phase are representative and do not depend on the chain length in any significant way.

III. NUMERICAL RESULTS AT $T=0$

A. Analytic estimation of the crossover from orbital polarons to itinerant electrons

The ground state of the orbital t-J model (1) depends on two parameters: J/t and $E_{\rm JT}/t$, and on hole doping $x=1-n$. We first investigate the ground state (at $T=0$) changing these parameters. A realistic value of $t\sim 0.4$–0.5 eV was estimated for manganites using the charge-transfer model.[20] Taking this as an energy unit, and the spectroscopic value for the energy of the high-spin excitation $\varepsilon(^6A_1)=U-3J_H\simeq 3.8$ eV, this leads to $J/t\simeq 1/8$. We will consider also $E_{\rm JT}>0$, which promotes localized behavior of e_g electrons.

At half filling one finds alternating $|x\rangle/|z\rangle$ orbitals in the ground state at $J>0$, with classical intersite correlations $T(n)=(-1)^n/4$. If a single hole is then doped to an orbitally ordered state at an $|x\rangle$ site, it can delocalize within a box consisting of three sites, as each neighboring $|z\rangle$ electron can interchange with the hole [see Fig. 1(a)]. This state is therefore favored over doping at the $|z\rangle$ site, and one can easily determine the energies of a doped hole in an antibonding and bonding state,

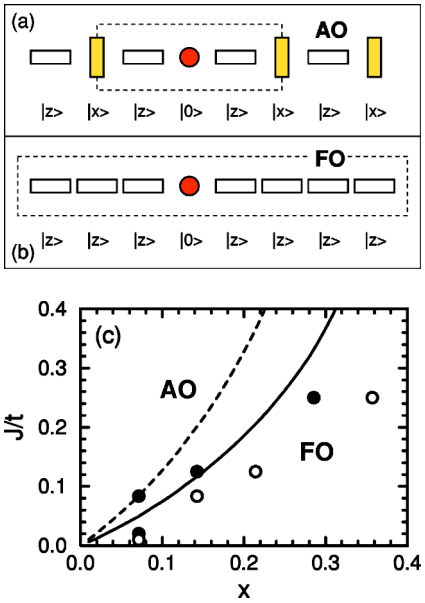

FIG. 1. (Color online) Competition between localized holes within an alternating orbital (AO) phase, with staggered localized $|x\rangle$ (shadded vertical boxes) and itinerant $|z\rangle$ (empty horizontal boxes) orbitals (a), and itinerant holes in ferro orbital (FO) $|z\rangle$ phase (b), in a 1-D chain along the c axis. A hole (shaded circle) is confined to a cluster of three sites in the AO state, while it is delocalized over the entire chain in the FO state, as indicated by dashed boxes. Part (c) shows a qualitative phase diagram of the 1-D orbital t-J model (6), with a critical concentration x_c separating the AO and FO phases, as obtained for $E_{\rm JT}=0$; and $\Delta=0$ (solid line), $\Delta=t$ (dashed line). Filled (empty) circles in (c) show the AO (FO) states found by exact diagonalization of an $N=14$ chain.

$$E_{1h,\pm}=\tfrac{1}{2}\overline{J}\pm\tfrac{1}{2}(\overline{J^2}+8t^2)^{1/2}, \tag{13}$$

with $\overline{J}=J+2E_{\rm JT}$ standing for an excitation energy of the configuration with a hole moved to a left (right) site within a three-site cluster shown in Fig. 1(a).

As long as the holes may be doped into separated three-site units (for $x\leqslant 0.25$), the total energy (per site) of an insulating phase follows from the weighted contributions of the undoped orbital ordered regions, and doped holes occupying the bonding states of individual clusters, with energy $E_{1h,-}$ (13),

$$E_I=-(1-x)E_{\rm JT}-(1-2x)J+xE_{1h,-}. \tag{14}$$

The energy of a metallic phase, which contains only itinerant $|z\rangle$ electrons for $n>0.5$ [see Fig. 1(b)],

$$E_M=\frac{1}{\pi}\int_{k<\pi/2}\varepsilon_{k,-}+\frac{1}{\pi}\int_{k<k_F}\varepsilon_{k,+}, \tag{15}$$

is obtained by integrating over the occupied one-particle band states $\varepsilon_{k,\pm}$. At finite $E_{\rm JT}$ one finds

$$\varepsilon_{k,\pm}=\pm\sqrt{E_{\rm JT}^2+4t^2\cos^2 k}. \tag{16}$$

The superexchange $\propto J$ does not contribute to E_M.

It is now of interest to compare the energy of two extreme situations: (i) an insulating phase with holes localized within three-site clusters [Eq. (14)], with (ii) a metallic (itinerant) phase [Eq. (15)]. One finds that at fixed J and $E_{\rm JT}=0$, an *insulator-metal transition* takes place when the hole concentration x increases. A critical concentration for this transition increases with increasing J/t [Fig. 1(c)]. The data points obtained from the exact diagonalization of an $N=14$ chain agree with the analytic estimation at $J/t=1/12$ and $1/8$, while for a larger value of $J/t=1/4$ the region of the insulating AO phase is more extended in the chain. Note, however, that the present analytic estimate is anyway only qualitative as the energy of the AO phase can be evaluated using a superposition of holes confined to three-site clusters only up to $x=0.25$. An extended region of stability of the AO phase results here from larger clusters of the itinerant phase which are still separated by immobile $|x\rangle$ states; such larger itinerant units occur already for $x<0.25$ at low values of J/t, as the gain in the kinetic energy for a hole moving within a larger cluster approaches fast the metallic limit with increasing cluster size, and may be easily compensated when a few exchange bonds are created. Indeed, the data show [see Fig. 1(c)] that the ground state for $x=1/14$ remains insulating with two $|x\rangle$ electrons at $J=0.02t$, and becomes metallic only for $J<0.02t$.

A simple estimation of the metal-insulator transition is also possible when a polaronic polarization around a hole[34] is included in Eq. (1),

$$H_\Delta=-\Delta\sum_i \overline{n_i}(\tilde{n}_{i-1,z}+\tilde{n}_{i+1,z}), \tag{17}$$

where $\tilde{n}_{jz}=\tilde{c}^\dagger_{i\pm1,z}\tilde{c}_{i\pm1,z}$ is the electron number operator in the restricted space without double occupancies, and $\overline{n_i}$ is a hole number operator (11). At $E_{\rm JT}=0$ a similar expression to Eq. (13) is then obtained, with $\overline{J}=J+\Delta$, and the range of an insulating AO phase shrinks in the phase diagram of Fig. 1(c). In fact, the polarization around doped holes is optimized in a metallic phase, and this result is special to the 1-D model. Therefore, we shall not consider this interaction further, as it gives qualitatively the same results as the orbital t-J model at $\Delta=0$, but with a somewhat reduced value of J.

At finite JT energy $E_{\rm JT}$ the situation changes in a drastic way. Even for relatively small $E_{\rm JT}\simeq 0.25t$ the AO phase is stabilized in the entire range of doping shown in Fig. 1(c). Note that even somewhat higher values could be more appropriate for realistic 3-D manganites.[34,39] This suggests that the JT effect may indeed play a very important role in manganites and stabilize an insulating phase with orbital order in a broad regime of doping; we address this question in Sec. III E.

B. Orbital order at half filling

The superexchange interaction in the orbital model (4) is Ising type, and therefore the orbital order in the undoped system at finite J is perfect, with alternating occupied $|x\rangle$ and $|z\rangle$ orbitals along the chain, and $\langle T_i^z T_{i+1}^z\rangle=-0.25$. The classical character of this ground state is reflected in the one-hole excitation spectra. If a single hole is added at half filling ($n=1$), it may be doped either at an $|x\rangle$ or at a $|z\rangle$ site. A hole doped at a $|z\rangle$ site is immobile and the energy of the final

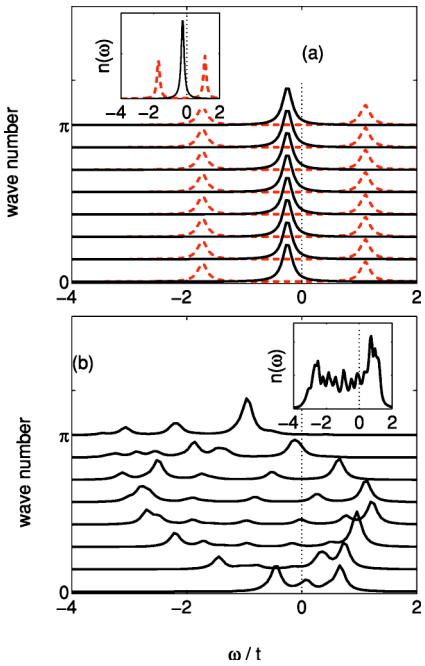

FIG. 2. (Color online) Spectral functions $A(k,\omega)$ at half filling for an $N=14$ site chain: (a) orbital model, with hole excitations within an occupied $|z\rangle/|x\rangle$ orbital shown by solid/dashed lines, respectively; (b) the spin t-J model. Insets show the density of states $n(\omega)$. Parameters: $J=0.125t$, $E_{\rm JT}=0$, $h_s=0$. We assumed a finite broadening of the peaks by $\delta=0.1t$.

state is higher by $2J$ than that of the initial state, as two exchange bonds are removed. This excitation appears as a localized peak at hole binding energy $-2J$ in Fig. 2(a). In contrast, when a hole replaces an $|x\rangle$ electron at site i, the resulting state is not an eigenstate of $\mathcal{H}_0$, the hole delocalizes over a three-site cluster including also occupied $|z\rangle$ orbitals at neighboring sites $i-1$ and $i+1$ [Fig. 1(a)], and the bonding and antibonding hole states (13) contribute. They give two maxima in the excitation spectrum of Fig. 2(a), with energies $E_{1h,\pm}-2J$. As the hole cannot hop over the sites occupied by $|x\rangle$ electrons, these two states are again localized within a cluster, and lead to k-independent maxima in the spectral function.

Strictly speaking, three-site terms, similar to those known from the derivation of the spin t-J model,[35] occur as well in the orbital model. One might expect that such terms, $\propto J\tilde{c}^{\dagger}_{i\pm1,z}\tilde{n}_{ix}\tilde{c}_{i\mp1,z}$, would change the spectral functions as a hole created at a $|z\rangle$ site could then hop to its second neighbors and interchange with immobile electrons in $|x\rangle$ orbitals. However, we have verified that these processes are of importance only for $J\sim t$, but do not lead to any significant changes of the spectral properties in the physically interesting regime of $J\lesssim 0.25t$. Therefore, they are neglected in what follows.

In contrast, the spectral functions obtained with the usual spin t-J model show a dispersive feature at the highest energy, a similar weaker dispersive feature at low energy, and incoherent spectral intensity between them [Fig. 2(b)]. The two dispersive features have a periodicity of π instead of 2π obtained for free electrons, are broadened and rather incoherent. Unlike in the 2-D case where a hole is trapped and can move only by its coupling to quantum fluctuations in the spin background, leading to a quasiparticle behavior with a dispersion on the energy scale $\propto J$,[40] the string potential is absent in a 1-D chain. The 1-D model shows spin-charge separation, because a hole may propagate after creating and leaving behind a single solitonic defect with two spins of the same direction next to each other.[41–43] However, the chain used in our case is too small for the spin-charge separation to be clearly visible. A more coherent component can be induced by introducing the coupling between the moving charge and spin fluctuations, which occurs in the presence of an external staggered field generating the string potential.[30,31] We address this issue in Sec. III E.

The present $N=14$ spin chain gives at half filling $\langle S^z_i S^z_{i+1}\rangle=-0.1491$, a value being already quite close to the exact result -0.1477 for an infinite Heisenberg chain. Therefore, we expect that the results presented for the more classical orbital chain with partly localized wavefunctions are at least of the same quality, and suffer even less from finite size effects.

C. Correlation functions at finite doping

First we consider the total energy $E_0=\langle\mathcal{H}_0\rangle$ as a function of the number of $|z\rangle$ electrons N_z at each doping x, and determine the actual distribution of e_g electrons in the ground state. The density of e_g electrons in two orbitals, n_x and n_z, depends on the ratio J/t. At half filling ($x=0$) one finds $n_x=n_z=0.5$, and the occupied orbitals alternate. At large $J/t\sim 1$ one expects that the orbital order is still close to perfect in the regions which separate orbital polarons, with the densities $n_z\simeq 0.5$ and $n_x\simeq 0.5-x$. On the contrary, in the limit of $J/t\to 0$ a single hole (in a finite chain) suffices to destabilize the orbital order, causing a transition to an itinerant (FO) state with $n_z=1-x$ and $n_x=0$.

The energy obtained for an $N=14$ chain filled by $9\leqslant N\leqslant 14$ electrons for two values of $J=0.25t$ and $0.125t$ are shown in Fig. 3. The tendency towards electron delocalization is quite distinct already for a higher value of $J=0.25t$, with the minimum of E_0 moving to $N_z>7$ with increasing doping x. The number of $|z\rangle$ electrons *increases* by one (to $N_z=8$) at the electron filling of $N_e=12$ and 11 electrons. At $N_e=10$ there remains just a single $|x\rangle$ electron which still blocks the hopping along the chain, while at $N_e=9$ all electrons are in $|z\rangle$ orbitals, and one obtains a metallic state. This transition to a metallic state is faster at a lower value of $J=0.125t$ [see also Fig. 1(c)]. Here adding a hole increases simultaneously the number of $|z\rangle$ electrons by one, and one finds $N_z=8$ and $N_z=9$ for $N_e=13$ and $N_e=12$, respectively, while doping by three holes gives already a metallic state with $N_z=N_e=11$.

The correlation functions in the ground state obtained after doping the chain by a single hole are very transparent at a higher value of $J=0.25t$, and are easily accessible by looking at the correlation functions (8)–(10). As shown schematically in Fig. 1(a), a hole replacing $|x\rangle$ electron is then confined to a three-site cluster, which can be deduced from the hole-orbital correlation function $P(n)$ [see Fig. 4(a)]. First of all,

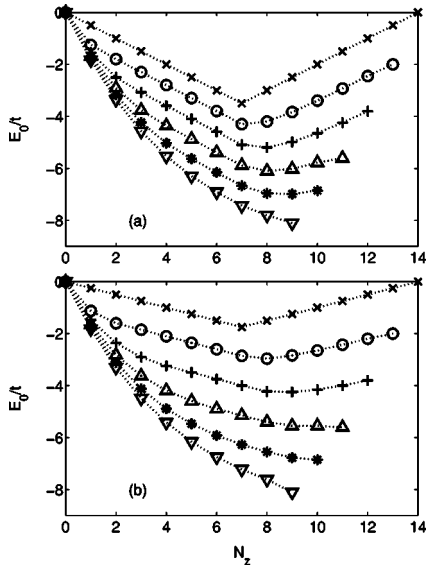

FIG. 3. Ground state energy E_0 as a function of the number of itinerant electrons N_z for 0 up to 5 holes (from top to bottom) added to a half-filled $N=14$ orbital chain, for $E_{\mathrm{JT}}=0$, and for (a) $J=0.25t$ and (b) $J=0.125t$.

at the nearest neighbor of a hole one finds preferably a $|z\rangle$ electron, with $P(1)<-0.25$ indicating that a hole spends more time at a central site than at either outer site of the three-site cluster [$P(1)=-0.25$ would correspond to the bonding state at $J=0$ and $P(1)=-0.5$ to a static hole at a central site]. This also causes a weak alternation of $P(n)$ with increasing n for further neighbors ($n\geqslant 2$). This result is different again from the spin t-J model, where almost no preference for the spin direction is found already at the nearest neighbor of a doped hole. Here the oscillations between even and odd neighbors are also much weaker as a hole is now delocalized, and one is averaging over several different configurations when $P(n)$ is evaluated. They correspond to the

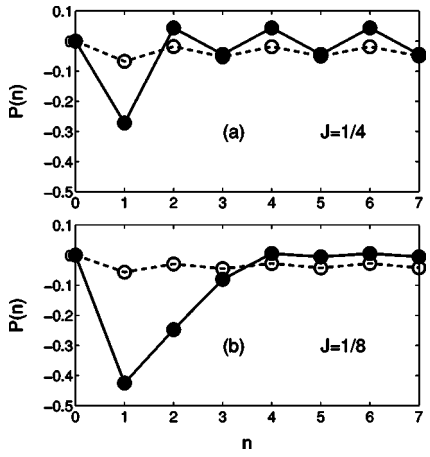

FIG. 4. Polarization of the orbital (filled circles, full lines) and spin (open circles, dashed lines) background $P(n)$ (8) at distance n from a single hole doped to a half-filled $N=14$ chain, as obtained for the ground state of the orbital/spin t-J model without staggered fields ($E_{\mathrm{JT}}=0$, $h_s=0$), and for (a) $J=0.25t$ ($N_z=7$), and (b) $J=0.125t$ ($N_z=8$).

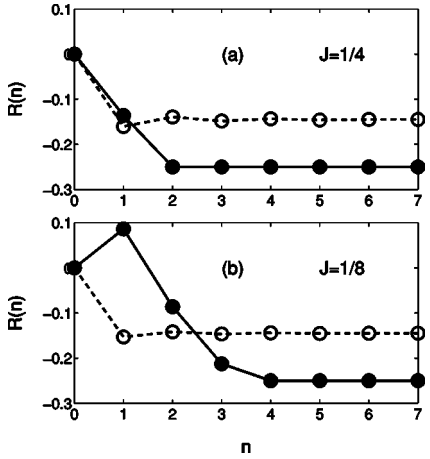

FIG. 5. Orbital correlations $R(n)$ (9) at distance n from a single hole doped to a half-filled $N=14$ chain (filled circles, full lines), as obtained for the orbital t-J model for $E_{\mathrm{JT}}=0$ and (a) $J=0.25t$ and (b) $J=0.125t$. Spin correlations obtained in the 1-D t-J model ($h_Q=0$) are shown for comparison by open circles and dashed lines.

domains with opposite spins, and weak oscillations result here only from holon-spinon correlations.

The ground state obtained for one hole at $J=0.125t$ is qualitatively different, as doping by one hole generates a single orbital flip and the number of itinerant $|z\rangle$ electrons increases to $N_z=8$. Figure 4(b) shows that this defect in the otherwise perfect orbital order occurs close to the hole, increasing the island over which the hole can delocalize, extending now over five sites. Hence, one finds $P(1)\simeq -0.44$ and $P(2)\simeq -0.25$, and only starting from the fourth neighbor this correlation is weakly positive. In contrast, a decreased value of J does not cause any significant change in the $P(n)$ correlations for the spin t-J model—they are only slightly weaker than for $J=0.25t$.

The orbital order, measured by second correlation function $R(n)$ (9), remains perfect at a sufficient distance from the doped hole, with $R(n)=-0.25$ [Fig. 5(a)]. In the case of a higher value of $J=0.25t$, the order is perfect starting from $n=2$, while for $J=0.125t$ with a larger island of the itinerant phase, it starts only at $n=4$. In addition, the orbital correlation $R(1)$ is here positive [Fig. 5(b)], as two $|z\rangle$ orbitals occur frequently next to each other both at the first and at the second neighbor of the hole which polarizes a larger five-site cluster. This behavior shows that phase separation occurs here in the regime of small J/t, and its mechanism which originates from orbital physics is completely different from that known from the spin t-J model at large $J/t>1$.

The spin t-J model has practically the same spin-spin correlations for both values of J. Due to quantum fluctuations in the Heisenberg 1-D chain, the correlation function $R(n)\simeq -0.14$ for $n>1$ [Fig. 5(a)] is much reduced from the classical value $R(n)=-0.25$ found for the orbital model. In fact, the long-range order is absent in the 1-D spin chain, and the quantum fluctuations contribute to the energy (per site), which is much lower than in the orbital case, $e_0=J\langle \vec{S}_i\cdot\vec{S}_{i+1}\rangle = 3J\langle S_i^z S_{i+1}^z\rangle$. The present $N=14$ spin chain gives at doping by one hole $\langle \overline{n_i} S_{i+n}^z S_{i+n+1}^z\rangle=-0.1448$ for $n=6,7$, a value which is

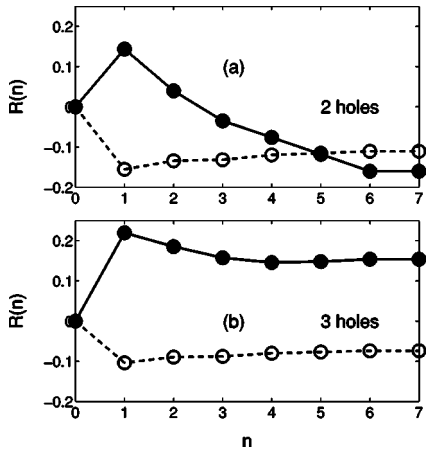

FIG. 6. Orbital correlations $R(n)$ (9) in a doped $N=14$ site chain (filled circles, full lines), as obtained for the orbital t-J model at $J=0.125t$, $E_{\rm JT}=0$ for doping by (a) two holes (insulating phase), and (b) three holes (metallic phase). Spin correlations are as in Fig. 5.

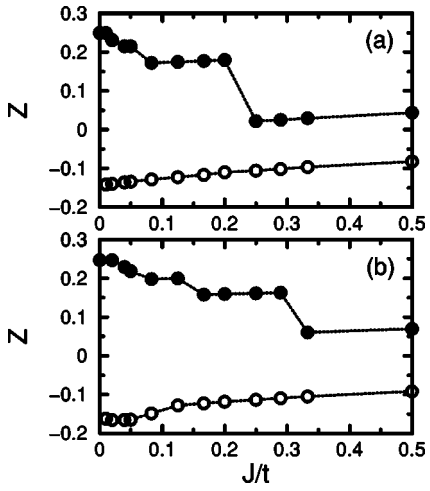

FIG. 7. Orbital and spin order (filled and empty circles) around a hole Z (10) as obtained for an $N=14$ chain with increasing J/t doped by (a) one hole and (b) two holes. Other parameters are as in Fig. 2.

only little reduced from -0.1491 found at half filling, showing that in spite of certain hole delocalization, spin intersite correlations are almost undisturbed by a single doped hole when the distance from it is sufficient.

When doping increases, a gradual crossover in $R(n)$ correlations towards a metallic chain with $|z\rangle$ orbitals occupied is found. The region doped by holes extends for two holes over nine sites and gives $R(n)<0$ starting from $n=3$ [Fig. 6(a)]. The correlation function $R(n)$ is averaged over several bonds, and the values of $R(n)\simeq -0.17$ for $n=6,7$ result from a superposition of the classical order ($\langle T_i^z T_{i+1}^z\rangle=-0.25$) in the insulating region and a positive value of $\langle T_i^z T_{i+1}^z\rangle$ correlations within the metallic cluster. When the insulating phase disappears at doping by three holes [Fig. 6(b)], $R(n)>0$ shows that only $|z\rangle$ orbitals are occupied. Three holes in the metallic phase avoid each other, and one finds a weak local minimum at $n=4$ in $R(n)$ correlations. The spin system gives instead negative $R(n)$, as here the hole hopping does not destroy the AF spin order. The correlation functions $R(n)$ for the spin t-J model have similar values for either two or three holes, while local minima found at $n=7$ and $n=4$ indicate again a characteristic distance between the holes in both cases.

The *polaronic* character of a doped hole is confirmed by the *positive* orbital correlation $Z>0$ between its neighbors (10). At $J\leqslant 0.01t$ the ground state is metallic and $Z=0.25$. Next, when J/t increases, the hole is first trapped in a large metallic cluster ($Z\simeq 0.22$), with its size gradually decreasing down to a five-site cluster when $J\geqslant 0.08t$—a hole is surrounded predominantly by two $|z\rangle$ electrons [Fig. 7(a)]. This ground state, with $N_z=8$ and $N_x=5$ electrons in the chain, remains stable up to $J=0.20t$. At $J/t>0.20$ the ground state changes again to $N_z=7$ and $N_x=6$ which gives a small orbital polaron [see Fig. 1(a)]. Due to finite superexchange energy J, the probability that the hole is in the center of a three-site cluster, with two neighboring $|z\rangle$ electrons, is somewhat higher than that it occupies either of side atoms, with one $|z\rangle$ and one $|x\rangle$ occupied orbital next to it. As a result, the correlation function $Z\simeq 0.02$ is now weakly positive. For the filling by two holes one has again five different ground states [Fig. 7(b)], with $Z=0.25$, $Z\simeq 0.22$, $Z\simeq 0.20$, $Z\simeq 0.16$, and $Z\simeq 0.07$ for increasing J/t. The transition to two separated three-site polarons occurs here at a somewhat higher value of $J\sim 0.30t$ than the transition to a single three-site polaron for the doping by one hole.

In contrast, the spin correlations between two hole neighbors are *negative* in the spin t-J model, both for one and for two holes (Fig. 7), showing the *solitonic* character of charge defect in the spin chain.[31] At low J/t these correlations are more pronounced, while increasing J/t leads to more delocalized holes and to weaker correlations $Z\simeq -0.10$ and $Z\simeq -0.12$ for the states doped either by one or by two holes at $J/t=0.1$. Somewhat stronger AF correlations in two-hole case confirm the solitonic character of charge defects in a 1-D spin chain, with a soliton compensated by an antisoliton.

D. Spectral functions at finite doping

Next we analyze the spectral functions obtained at finite doping. Starting from the ground state of an orbital chain with a single hole, we found that in the region of very small J ($J\sim 0.01t$ for an $N=14$ chain) the spectral function of the orbital model shows a free propagation of a hole within the entire chain, and electrons fill $|z\rangle$ orbitals. This case (not shown) is however only of theoretical interest, and at $J\simeq 0.125t$, adequate for $LaMnO_3$, one finds instead fairly localized spectra [Fig. 8(a)]. One recognizes the maxima which correspond to localized $|x\rangle$ excitations at $\omega-\mu\simeq -1.8t$, and the structures corresponding to the bonding and antibonding states of the $|x\rangle$ excitations at $\omega-\mu\simeq -3.3t$ and $-0.3t$. The spectra are k dependent and the spectral weight moves to higher energies with increasing momentum k, following the tight-binding dispersion at $E_{\rm JT}=0$, $\epsilon_{k-}=-2t\cos k$ (16). The total widths of the spectrum in Fig. 8(a) is close to $4t$, i.e., to full free-electron dispersion obtained for electrons in $|z\rangle$ orbitals.

The spectrum obtained for spin t-J model is drastically different. A broadened quasiparticle band crossing the Fermi

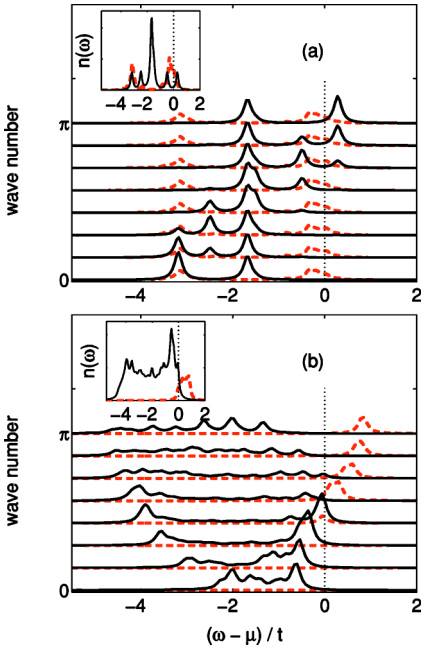

FIG. 8. (Color online) Spectral functions $A(k,\omega)$ for $N=14$ chains doped with one hole for $J/t=0.125$: (a) orbital t-J model (1) with $N_z=8$ and $N_x=5$—solid and dashed lines for $|z\rangle$ and $|x\rangle$ excitations; (b) spin t-J model (12) with $N_\uparrow=6$ and $N_\downarrow=7$—solid and dashed lines for hole and electron excitations. Insets show the densities of states $n(\omega)$. Other parameters and peak broadening as in Fig. 2.

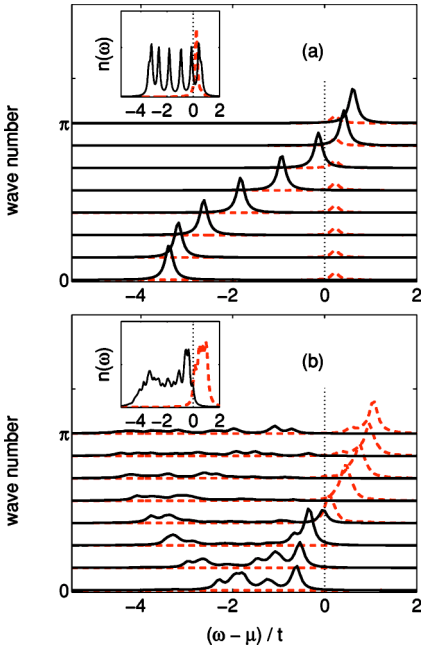

FIG. 9. (Color online) Spectral functions $A(k,\omega)$ for $N=14$ chains doped with three holes for $J/t=0.125$: (a) orbital t-J model (1) with $N_z=11$ and $N_x=0$, (b) spin t-J model (12) with $N_\uparrow=5$ and $N_\downarrow=6$. The meaning of solid (dashed) lines, insets and other parameters are the same as in Fig. 8.

energy resembles a tight-binding dispersion with a reduced bandwidth [Fig. 8(b)]. For low momenta k, where a larger system would show spin-charge separation, the spectra are especially incoherent. Most of the spectral intensity is in the incoherent part, but one recovers a coherent propagation in the limit of $J\to 0$, which occurs in this case without polarizing the chain, as both spin flavors are mobile in this limit and the spin direction is irrelevant.

As we have shown in Fig. 3(b), doping $N=14$ chain by three holes is sufficient for the crossover to the metallic state for a realistic value of $J/t=1/8$. The spectral function $A(k,\omega)$ confirms the metallic behavior of the orbital chain for this filling, and the excitations in $|x\rangle$ orbitals contribute with a k-independent maximum only above the Fermi energy [Fig. 9(a)]. In contrast, the spectral functions in the spin t-J model [Fig. 9(b)] are qualitatively very similar to those found at lower doping by one hole [Fig. 8(b)], but with more weight transferred now to the quasiparticle states above the Fermi energy μ at $k>\pi/2$. The weight of the quasiparticle states for $\omega>\mu$ is enhanced, while the incoherent spectral weight is decreased for these values of k.

The ground state of the orbital chain is insulating at a larger value of $J=0.25t$ [Fig. 3(a)]. Therefore, the spectral functions consist in this case of several incoherent features for each k value, with the first moment of the spectra following again the single-particle dispersion (Fig. 10). The incoherent feature at $\omega\simeq\mu$, originating from excitations within $|x\rangle$ orbitals, is partly below the Fermi energy. This part of the spectral weight follows from $|x\rangle$-hole excitations which are still possible at the filling by $N_z=9$ and $N_x=2$ electrons.

E. Polarons induced by the JT effect

The energies of the insulating and metallic phase are close to each other for typical parameters. Therefore, even a moderate JT energy $E_{\rm JT}=0.25t$ is sufficient to stabilize the insulating phase in a broad regime of doping, with occupied $|x\rangle$ orbitals fragmenting the chain into smaller units. When a single hole is doped, the JT field has qualitatively a similar effect as a larger value of J—a hole is then well localized within a three-site cluster, and the hole-orbital correlation $P(n)$ exhibits more pronounced alternation, indicating a robust orbital order [Fig. 11(a)], as in Fig. 5(a). The orbital intersite correlations $R(n)$ are perfect already beyond the second nearest neighbor of the hole [Fig. 11(b)].

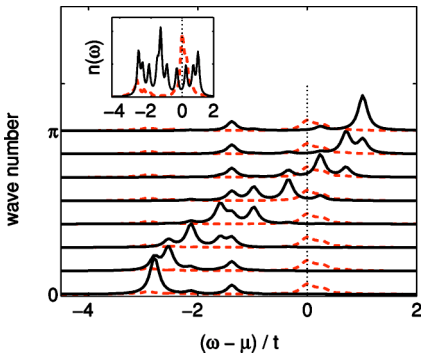

FIG. 10. (Color online) Spectral functions $A(k,\omega)$ for an $N=14$ orbital chain doped with three holes for $J/t=0.25$. Solid and dashed lines for $|z\rangle$ and $|x\rangle$ excitations. Inset, other parameters and peak broadening as in Fig. 2.

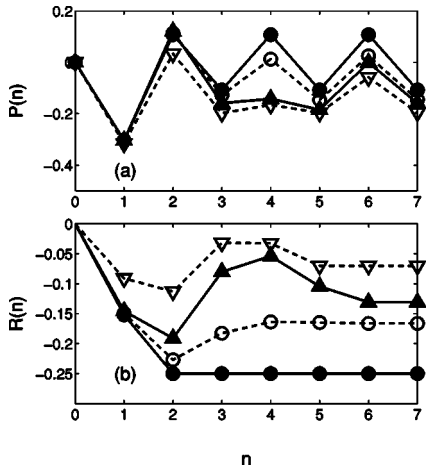

FIG. 11. Evolution of orbital correlations with increasing hole doping, as obtained for $J=0.125t$ and $E_{\rm JT}=0.25t$: (a) hole-orbital correlations $P(n)$, and (b) hole-orbital-orbital correlations $R(n)$. Filled circles, empty circles, filled triangles, and empty triangles for one, two, three, and four holes doped to an $N=14$ orbital chain.

When more holes are added, the orbital order gradually softens, but a clear tendency towards orbital alternation is observed even for high doping with four holes [Fig. 11(b)]. Note that a second hole may be added at a fourth or sixth site away from the first one. This, together with weak hole hopping within the three-site clusters, weakens both hole-orbital correlations $P(n)$ and the orbital order $R(n)$ at $n=4$ and (less) at $n=6$. For the present case of $N=14$ sites these latter correlations are reduced more for $n\geqslant 4$ than for $n=2$. With a third hole added, we found separated holes in three-site clusters, with each hole occupying predominantly the central site of its cluster in order to minimize the JT energy. A typical interhole distance is then four lattice constants, and for this reason $P(4)$ becomes negative, and $R(4)$ is reduced stronger than $R(n)$ for any other $n>0$. The fourth hole is added at one of $|x\rangle$ orbitals within a longer $|z\rangle-|x\rangle-|z\rangle-|x\rangle-|z\rangle$ unit, and makes then the first bigger cluster, with two holes and three mobile $|z\rangle$ electrons. Particularly in this regime of parameters and up to this doping regime, the distribution of holes is reminiscent of doping CuO_3 chains in $YBa_2Cu_3O_{6+x}$, where holes are doped first in separated CuO_2 units, where they are trapped, generating fragmented units of CuO_3 chains and causing jumps and plateaus for the hole counts in the CuO_2 planes as a function of doping.[44]

The spectral functions $A(k,\omega)$, presented for two representative doping levels with one and three holes in Fig. 12, show that they are remarkably similar in the entire regime of doping $x<0.3$. Excitations in $|x\rangle$ orbitals lead to maxima below and above the Fermi energy, with the spectral weight moving gradually to higher energies under increasing doping. For hole excitations in $|z\rangle$ orbitals one finds three nondispersive features: the central peak for doping within the orbital ordered regions, and two side peaks at energies corresponding to the excitations of orbital polarons. The spectral weight of the latter features increases on the cost of the central peak when doping increases, and the spectral weight distribution depends on momentum k. At doping increasing up to five holes (not shown) the spectra are still fairly localized,

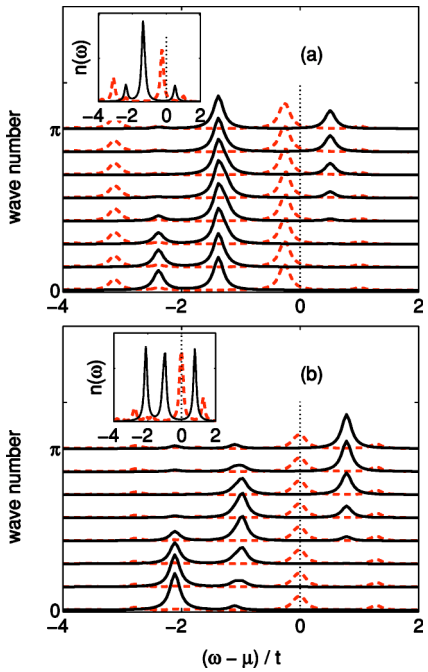

FIG. 12. (Color online) Spectral functions $A(k,\omega)$ for an insulating $N=14$ orbital chain for $J/t=0.125$ and $E_{\rm JT}=0.25t$, obtained for increasing doping by (a) one hole, and (b) three holes. Solid and dashed lines for $|z\rangle$ and $|x\rangle$ excitations. Insets and peak broadening are as in Fig. 2.

and the $|x\rangle$ spectral weight is further reduced for $\omega<\mu$.

A remarkable change of the spectral functions $A(k,\omega)$ has been found for the spin t-J model in the presence of a finite staggered field $h_s=2J$. The field generates a string potential, and simulates thus a 2-D model.[31] However, in this quantum model, in contrast to the orbital model shown in Fig. 12(a), a hole is not confined within a polaron but can move coherently when it couples to quantum spin fluctuations, which repair the defects in the spin background generated by a moving hole. As a result, a quasiparticle peak emerges close to the Fermi energy (Fig. 13), indicating a propagation of a hole dressed by spin excitations, with a dispersion $\sim 4J$ [note the units in Eq. (12)]. The remaining spectral weight is dis-

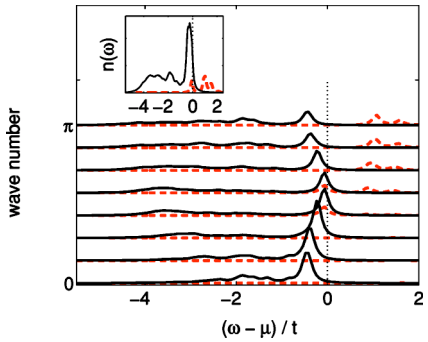

FIG. 13. (Color online) Spectral functions $A(k,\omega)$ for an $N=14$ spin t-J chain (12) at doping by one hole, as obtained for $J/t=0.125$ with a staggered field $h_s=2J$. Solid and dashed lines indicate hole and electron excitations. The inset shows the density of states $n(\omega)$.

tributed over incoherent features at lower energy while the low energy quasiparticle band visible in Fig. 8 has vanished, as well as the incoherence of the band for small k.

Moreover, the quasiparticle band has lost a simple tight-binding-like dispersion found before at $h_s=0$, and instead of crossing the Fermi energy, it has periodicity π because of the doubled unit cell and folds back toward lower energies after reaching the Fermi energy at $k=\pi/2$. The peaks are sharpest near this point, confirming the quasiparticle character of this excitation, but have lower spectral weight at $k=\pi$ than at $k=0$. The quasipartiple band close to the Fermi energy leads to a quite distinct peak in the density of states (see the inset of Fig. 13). It is separated by a pseudogap from the electronic excitations at $\omega>\mu$, and also by another pseudogap at $\sim 4J$ below the Fermi energy from the incoherent part of the spectrum at lower energies. Thus, the present case is radically different from the case of $h_s=0$ [see Fig. 2(b)], and resembles the spectral functions for a 2-D spin t-J model.[29,40]

IV. ORBITAL POLARONS AT FINITE TEMPERATURE

A. Effective orbital t-J model

At increasing temperature the FM spin order assumed in Sec. II is gradually destroyed and AF spin configurations on the bonds occur with finite probability, modifying the form of both t and J terms in Eq. (1). Even when the ground state at $T=0$ is FM, superexchange interactions which originate from t_{2g} electron excitations play an important role and contribute at finite temperature. These interactions are frequently treated as an effective AF superexchange between core $S=3/2$ spins, but *de facto* they depend on the total number of d electrons of two interacting Mn ions.[14] We have verified, however, that the t_{2g} superexchange terms derived for these different configurations are of the same order of magnitude, so it is acceptable to consider their effect as equivalent to a Heisenberg interaction with an average exchange constant $J'>0$. Therefore, we include in the present 1-D model the spin interaction,

$$H_{J'}=J'\sum_i(\vec{S}_i\cdot\vec{S}_{i+1}-S^2). \tag{18}$$

The superexchange due to e_g electron excitations contains spin scalar products multiplied by orbital interactions on the bonds, and the full many-body problem would require treating the coupled spin and orbital dynamics. Here we decouple spins and orbitals in the mean-field approximation, and study the orbital correlations and their consequences for the magnetic order by replacing the scalar products of spin operators on each bond by their average values,[1,5]

$$\langle\vec{S}_i\cdot\vec{S}_{i+1}\rangle=S^2(2u_{i,i+1}^2-1), \tag{19}$$

where $u_{i,i+1}=\cos(\theta_{i,i+1}/2)e^{i\chi_{i,i+1}}$, and directions of two classical spins at sites i and $i+1$ differ by angle $\theta_{i,i+1}$. The complex phase $\chi_{i,i+1}$ does not have any effect on the present 1-D model.[10]

We investigate the *effective orbital t-J model*,

$$\mathcal{H}(\mathcal{S})=H_t+H_J+H_{J'}+H_{\rm JT}, \tag{20}$$

where the AF interactions of core spins (18) and the JT field acting on orbital variables (6) are playing the role of external fields. The hopping term H_t describes the dynamics of e_g electrons which are locally coupled to t_{2g} core spins by a large Hund's exchange J_H element, and have their spins parallel to them in the ground state. In agreement with double exchange mechanism,[3,13] the hopping amplitude along each bond $\langle i,i+1\rangle$ is then modified by the spin order to

$$\tilde{t}_{i,i+1}=tu_{i,i+1}, \tag{21}$$

and vanishes when the spins are antiparallel. This approximation allowed us to establish the existence of magnetic polarons in the 1-D Kondo model.[11]

The superexchange due to e_g electrons $\propto J$ generates orbital interactions in H_J which follow from virtual charge excitations, either for Mn^{3+}-Mn^{3+} or for Mn^{3+}—Mn^{4+} pairs. Consider first the spin-orbital model of Ref. 20 for an undoped $LaMnO_3$. So far, we included the orbital superexchange [Eq. (4) for a situation when high-spin e_g excitations dominate, but low-spin excitations would also contribute at finite temperature. Taking realistic parameters for the Coulomb interaction U and Hund's exchange J_H, the low-spin $^4A_1$, ^4E, and $^4A_2$ states have the energies 7.3, 7.8, and 9.6 eV.[20] We keep the relative importance of various excitations and write the terms resulting from various charge excitations to the superexchange, after averaging them over the spin configuration, as follows:

$$\begin{aligned}
&\frac{1}{10}\frac{t^2}{\varepsilon(^6A_1)}\langle\vec{S}_i\cdot\vec{S}_{i+1}+6\rangle=\frac{J}{5}(4u_{i,i+1}^2+1),\\
&\frac{1}{16}\left[\frac{t^2}{\varepsilon(^4A_1)}+\frac{3}{5}\frac{t^2}{\varepsilon(^4E)}\right]\langle\vec{S}_i\cdot\vec{S}_{i+1}-4\rangle\simeq\frac{J}{5}(u_{i,i+1}^2-1),\\
&\frac{1}{16}\left[\frac{t^2}{\varepsilon(^4E)}+\frac{t^2}{\varepsilon(^4A_2)}\right]\langle\vec{S}_i\cdot\vec{S}_{i+1}-4\rangle\simeq\frac{9J}{20}(u_{i,i+1}^2-1).
\end{aligned} \tag{22}$$

In a doped system one finds only AF superexchange terms for Mn^{3+}—Mn^{4+} bonds [while FM ones are explicitly included as double exchange in the orbital model (20)], which contribute only if an e_g electron at site Mn^{3+} occupies a directional orbital along the considered bond direction, in our case a $3z^2-r^2$ orbital, and can hop to its Mn^{4+} neighbor. Taking the excitation energy to the low-spin configuration $\varepsilon(^3E)\simeq 3$ eV,[14] one finds

$$\frac{1}{8}\frac{t^2}{\varepsilon(^3E)}\langle\vec{S}_i\cdot\vec{S}_{i+1}-3\rangle\simeq J(u_{i,i+1}^2-1). \tag{23}$$

Using the coefficients given in Eqs. (22) and (23), one arrives at the effective orbital t-J model (20), with

$$H_t=-\sum_i\tilde{t}_{i,i+1}(\tilde{c}_{iz}^\dagger\tilde{c}_{i+1,z}+\tilde{c}_{i+1,z}^\dagger\tilde{c}_{iz}), \tag{24}$$

$$H_J = \frac{1}{5}J\sum_i (2u_{i,i+1}^2+3)\left(2T_i^zT_{i+1}^z-\frac{1}{2}\tilde{n}_i\tilde{n}_{i+1}\right) - \frac{9}{10}J\sum_i (1-u_{i,i+1}^2)\tilde{n}_{iz}\tilde{n}_{i+1,z} - J\sum_i (1-u_{i,i+1}^2) \times[\tilde{n}_{iz}(1-\tilde{n}_{i+1})+(1-\tilde{n}_i)\tilde{n}_{i+1,z}]. \quad (25)$$

The hopping (H_t) and the interaction (H_J) terms depend on the actual spin configuration which fixes the bond variables $\{u_{i,i+1}\}$ [see Eq. (19)]. In the FM state at $T=0$ all $u_{i,i+1}=1$, the AF terms vanish, and one recovers the form of H_t and H_J used in Sec. II.

It is a crucial feature of the effective orbital model given by Eq. (20) that spin interactions are influenced by orbital correlations along the chain, and the latter can support either FM (for alternating x/z orbitals) or AF (for polarized z orbitals) spin order. At $T=0$ one can find on optimal state by minimizing the total (internal) energy of the system, $E=\langle\mathcal{H}(\mathcal{S})\rangle$, over the spin and orbital configurations. In fact, at $T=0$ two solutions are possible, depending on the parameters in Eq. (20). Let us consider first a purely electronic model with $E_{\rm JT}=0$ at half filling (we will show below that the situation is similar at $E_{\rm JT}>0$, but the region of stability of the FM states is extended). If $J'=0$, the FM order is stable and coexists with alternating orbital order. This situation was discussed in detail in Sec. III. However, a relatively small value of $J'=0.0125t$ is sufficient to compensate the energy difference between this state and an AF state with occupied $|z\rangle$ orbitals, and (at $T=0$) one finds the latter state for $J'>0.0125t$. It is interesting to investigate a competition between these magnetic states at finite temperature when the chain is doped.

We investigated the spin and orbital correlations for the effective orbital t-J model (20) at finite temperatures by employing a combination of a Markov chain Monte Carlo (MCMC) algorithm for the core spins, with Lanczos diagonalization for the many-body problem posed by the orbital chain of $N=12$ sites with periodic boundary conditions, at each given distribution of classical variables $\{u_{i,i+1}\}$ for $i=1,\ldots,12$, which stands for a particular spin configuration. The partition function to then be evaluated is

$$\mathcal{Z}=\int \mathcal{D}[\mathcal{S}]\mathrm{Tr}_c e^{-\beta\mathcal{H}(\mathcal{S})}, \quad (26)$$

where $\beta=1/k_BT$ (we adopt the units with $k_B=1$), and $\int\mathcal{D}[\mathcal{S}]$ denotes the integral over the N-dimensional space of all core spin configurations for the chain of length N. The core spins $\mathcal{S}\equiv\{\vec{S}_i\}$ determine the site-dependent hopping parameters $\{u_{i,i+1}\}$ and thus the fermionic Hamiltonian $\mathcal{H}(\mathcal{S})$ is fixed.

The trace over the fermionic degrees of freedom, $\mathrm{Tr}_c\, e^{-\beta\mathcal{H}(\mathcal{S})}=:w(\mathcal{S})$, gives the statistical weight for $\mathcal{S}$ and is sampled by the MCMC. For independent electrons it can easily be evaluated;[5,6] for interacting electrons one has to use a Lanczos algorithm,[11] but as $w(\mathcal{S})$ is strictly positive, one still has no sign problem. Since the position of the $|x\rangle$ electrons is conserved, the Hamiltonian (20) has a block-diagonal structure, with each block corresponding to one fixed distribution of $|x\rangle$ electrons along the chain. There are, of course, many such blocks, but their subsequent diagonalization is still much faster than the diagonalization of the complete matrix. For the extreme case of the completely filled chain, each block has dimension one, meaning that the Hamiltonian is already diagonal and no matrix-vector multiplication has to be performed. Furthermore, degenerate eigenvalues can be resolved, if they are in different blocks.

For the MCMC updates, $w(\mathcal{S})$ was calculated from the lowest few eigenenergies of *each* block for an $N=12$ chain, until a new Lanczos step did no longer modify the contribution from this block. Observables were only calculated from the lowest 14 eigenstates of the *whole* space. In order to monitor this approximation, the Boltzmann factor of these states was measured. The weight of the highest included state was approximately 1.5 percent for the worst case (filled chain, $\beta t=20$, $J'=0.02$, $E_{\rm JT}=0$), 0.3–0.5 percent for $\beta t=50$ and the filled chain and negligible for $\beta=100$ or finite doping. This means that for those observables, which are calculated from the eigenstates of the Hamiltonian, at most a few percent of the total weight were missed. For the MCMC updates and for observables which do not need the eigenvectors (core spin correlation and total number of $|x\rangle/|z\rangle$ electrons), the error was even smaller.

The core spins were rotated for whole sections of the chain at once. Because acceptance for core spin updates was high, we performed two or three such rotations before testing acceptance. Every spin was therefore rotated several times per sweep. The numbers N_x and N_z of $|x\rangle$ and $|z\rangle$ electrons remained fixed for the evaluation of $w(\mathcal{S})$, and every five updates we proposed to increase (decrease) N_x and decrease (increase) N_z, respectively, thereby sampling N_x and N_z. The total number of electrons N_e was kept fixed. Between measurements, 40 to 100 lattice sweeps (depending on temperature) were done in order to decorrelate the samples. We then employed autocorrelation analysis and found the samples to be uncorrelated. To reduce the statistical errors, 200 uncorrelated samples were obtained for each set of parameter values.

B. Orbital order versus spin order

In addition to the correlation functions studied in Sec. III, spin correlations $\langle S_i^zS_j^z\rangle$ are now investigated by evaluating the spin structure factor,

$$S(k)=\frac{1}{N^2}\sum_{ij} e^{ik(R_i-R_j)}\langle\vec{S}_i\cdot\vec{S}_j\rangle, \quad (27)$$

which depends on the 1-D momentum k, and follows from Monte Carlo simulations of $N=12$ chains. The averages $\{\langle\vec{S}_i\cdot\vec{S}_j\rangle\}$ are calculated from the spin configurations $\mathcal{S}\equiv\{\vec{S}_i\}$ determined by the MCMC updates for $\{u_{i,j}\}$ — these quantities are related to each other as in Eq. (19).

The interplay between spin and orbital correlations becomes transparent by varying the core spin AF superexchange J' (18) due to t_{2g} electrons. We investigated spin and orbital order for two characteristic values of temperature: $\beta t=100$ and $\beta t=50$, corresponding to $T\sim 60$ and ~ 120 K

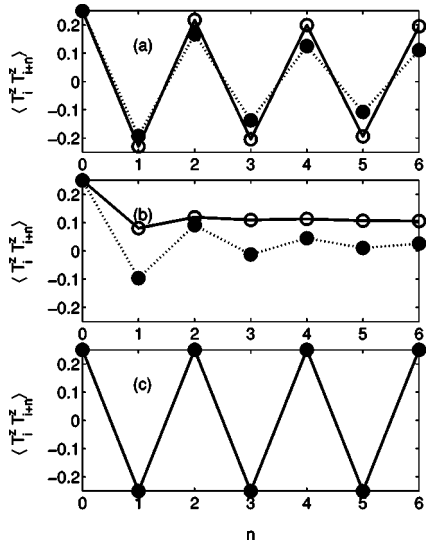

FIG. 14. Orbital correlations $\langle T_i^z T_{i+1}^z \rangle$ (7) at half filling, as obtained at low ($\beta t=100$, open circles), and at intermediate ($\beta t=50$, filled circles) temperature for $N=12$ site orbital chain (20), with $J=0.125t$, and (a) $J'=E_{\rm JT}=0$, (b) $J'=0.02t$, $E_{\rm JT}=0$, and (c) $J'=0.02t$, $E_{\rm JT}=0.25t$. Statistical errors are smaller than the symbol sizes.

for $t\sim 0.5$ eV, i.e., well below the magnetic transition. First we consider the case of $J'=0$ which reproduces the ground state analyzed in Secs. II and III. While the orbital alternation, measured by $T(n)$ correlation function (7), is perfect at $T=0$, it softens somewhat when temperature increases, but is still robust at temperature $\beta t=50$, as shown in Fig. 14(a). Orbital alternation supports the FM spin order at half filling, which gives a distinct maximum at $k=0$ of the spin structure factor $S(k)$ (see Fig. 15). In the weak doping regime with one or two holes added, the spin correlations, $\langle n_i S_{i+n}^z S_{i+n+1}^z \rangle$, are driven by superexchange and are FM at any distance n from the hole, and only weakly depend on n. These correlations increase by a factor close to two when the doping changes from two to three holes. This explains why the maximum of $S(k)$ at $k=0$ remains almost unchanged in the low doping regime by one or two holes, but is next strongly enhanced when doping increases to three holes. Precisely at this concentration electrons redistribute within the chain and occupy practically only $|z\rangle$ orbitals, giving a metallic state. This demonstrates that double exchange plays a primary role in the observed insulator-metal transition and significantly enhances the stability of the FM order in the metallic phase.

At $J'=0.02t$ the orbital correlations found in the half-filled chain are markedly different [Fig. 14(b)]. At low temperature ($\beta t=100$) they indicate that primarily (but not only) $|z\rangle$ orbitals are occupied, while no $|x\rangle$ electrons were found in the ground state at $T=0$. This orbital state is induced by finite J', and supports the AF spin interactions due to e_g excitations which select then low-spin states in the e_g excitations along $|z\rangle-|z\rangle$ bonds. When a single hole is doped, the spin correlations remain still AF at low temperature [Fig. 16(a)], except for the spin-spin correlation between the site occupied by the hole and its nearest neighbor, giving rise to a small FM polaron. Therefore, the value of $S(0)$ increases already at

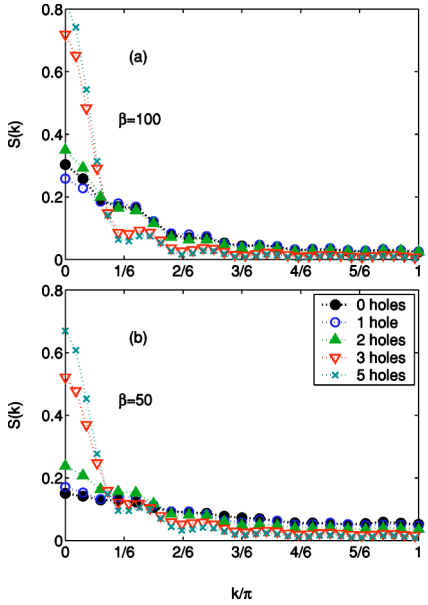

FIG. 15. (Color online) Spin structure factor $S(k)$ as obtained for a half-filled $N=12$ orbital chain (20), and for increasing hole doping up to five holes: (a) at low temperature $\beta=100$, and (b) at intermediate temperature $\beta=50$ (in units of t^{-1}). Statistical errors are smaller than the symbol sizes. Parameters: $J=0.125t$, $J'=0$, $E_{\rm JT}=0$.

this low doping, and the electron density in $|z\rangle$ orbitals is enhanced close to the hole itself.

When temperature increases, it becomes clear that the orbital $|x\rangle/|z\rangle$ alternation, supporting the FM spin interactions, competes at half filling with the above uniformly polarized chain with occupied $|z\rangle$ orbitals, supporting the AF spin order. A clear tendency towards orbital alternation is detected by a negative nearest-neighbor orbital correlation $T(1)\simeq -0.10$ [Fig. 14(b)] at higher temperature ($\beta t=50$). Al-

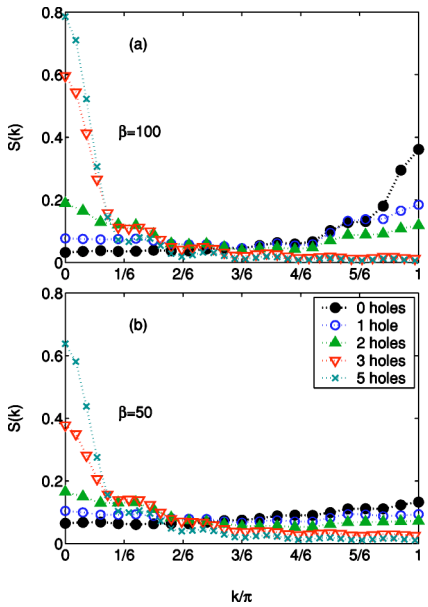

FIG. 16. (Color online) Spin structure factor $S(k)$ for an $N=12$ orbital chain (20) as in Fig. 15, but for $J'=0.02t$.

TABLE I. The total number of electrons in itinerant orbitals N_z (top part) and in localized orbitals N_x (bottom part) for different doping level x and for increasing temperature βt, as obtained in the Monte-Carlo simulations for an $N=12$ orbital chain [Eq. (20)] (statistical errors are also given). Parameters: $J=0.125t$, $J'=0.02t$, $E_{\rm JT}=0$.

			N_z	
βt	$x=0$	$x=1/12$	$x=1/6$	$x=1/4$
100	9.97±0.09	9.80±0.06	9.64±0.04	9.0±0.0
50	7.85±0.07	8.51±0.06	8.81±0.04	8.98±0.01
30	7.47±0.07	8.05±0.06	8.53±0.05	8.88±0.03
20	7.34±0.07	7.85±0.06	8.18±0.06	8.55±0.04
			N_x	
βt	$x=0$	$x=1/12$	$x=1/6$	$x=1/4$
100	2.03±0.09	1.20±0.06	0.36±0.04	0.0±0.0
50	4.15±0.07	2.49±0.06	1.19±0.04	0.02±0.01
30	4.53±0.07	2.95±0.06	1.47±0.05	0.12±0.03
20	4.66±0.07	3.15±0.06	1.82±0.06	0.45±0.04

though the value of $S(\pi)$ is still larger than $S(0)$ at half filling, both (weak) maxima, corresponding to FM and AF order, become almost equal already for doping with one hole [Fig. 16(b)]. This case is qualitatively similar to a chain doped by two holes at $\beta t=100$ [Fig. 16(a)], where also two (stronger) maxima of $S(k)$ indicate coexisting islands of FM and AF spin correlations along the chain. Thus, we found that the AF correlations are gradually changed into FM ones with increasing temperature. This trend follows from the difference in the energy scales—when the thermal magnetic excitations destroy the energy gains due to J and J', the kinetic energy $\propto t$ is a dominating energy which can be optimized by selecting $|z\rangle$ occupied orbitals and FM spin correlations.

At doping by three holes the spin correlations are FM, both at low ($\beta t=100$) and at higher temperature ($\beta t=50$), showing that the double exchange enhances the effective FM interactions and changes the characteristic temperature at which the spin correlations weaken—thus the Curie temperature T_C would increase in a 3-D case. This agrees with the experimental observations—indeed, the Curie temperature increases with hole doping x in the metallic regime.[24,45]

Although at $T=0$ one finds indeed the AF ground state with $N_z=12$ for a half-filled $N=12$ chain, many excited states with a few $|x\rangle$ orbitals occupied are found at low energy and contribute already at $\beta t=100$. As a result, electrons are redistributed over e_g orbitals by thermal excitations, and the orbital polarization at $\beta t=100$ is far from complete, with $N_z\simeq 10$ and $N_x\simeq 2$ (Table I). When temperature increases further to $\beta t=50$ ($\beta t=20$), orbital disorder increases and one finds $N_z\simeq 7.8$ and $N_x\simeq 4.2$ ($N_z\simeq 7.3$ and $N_x\simeq 4.7$). This demonstrates that the balance between FM and AF terms realized at half filling is rather subtle—increasing temperature favors more disorder in the chain which destroys a uniform AF phase, supported by charge excitations along $|z\rangle -|z\rangle$ bonds.

The population of localized $|x\rangle$ states in the chain decreases quite fast with doping, particularly in the regime of $\beta t\leqslant 100$. At $x=1/4$ one finds almost no $|x\rangle$ defects in the metallic chains, except at rather high temperature $\beta t=20$. Increasing electron density in $|x\rangle$ orbitals with increasing temperature may be seen as a precursor effect for the metal-insulator transition at T_C in the intermediate doping regime.

C. Polaronic features at finite doping

The spectral functions $A(k,\omega)$ obtained for the FM phase at half filling for $J'=0$ (not shown) are similar to those discussed in Sec. III D. Apart from some broadening due to finite T, the one-hole excitations are again fairly localized, similar to those shown in Fig. 2. In the doped regime one finds first the localized spectra at low doping, similar to those of Fig. 8(a), with a distinct pseudogap at the Fermi energy μ. As found before at $T=0$, doping by three holes suffices for the crossover to the metallic phase, with somewhat broadened peaks in $A(k,\omega)$, following the one-particle dispersion due to the hopping within $|z\rangle$ orbitals, like in Fig. 9(a).

In contrast, the spectral properties obtained for the AF phase found at half filling with $J'=0.02t$ are quite different (Fig. 17). First of all, there are predominantly $|z\rangle$ electrons at low temperature $\beta t=50$, and still moreso at $\beta t=100$, so the

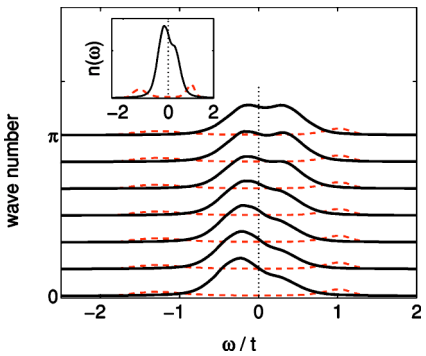

FIG. 17. (Color online) Spectral functions $A(k,\omega)$ for a half-filled $N=12$ orbital chain (20) at temperature $\beta t=100$. Solid and dashed lines for $|z\rangle$ and $|x\rangle$ excitations. The inset shows the density of states $n(\omega)$. Parameters: $J=0.125t$, $J'=0.02t$, $E_{\rm JT}=0$.

spectral weight of the localized $|x\rangle$ hole excitations, found at energies $\omega\sim-1.3t$ and $\sim t$ [Fig. 14(b)], appears to be very low. The $|z\rangle$ excitations have an insulating character and are incoherent. They are given by a superposition of two features, namely a dispersionless peak at the hole binding energy $\omega\sim-2J$ and a weakly dispersive band with bandwidth $\sim 0.5t$. The first feature stems from the few $|z\rangle$ electrons which are surrounded by $|x\rangle$ electrons and is similar to that discussed in Sec. III B. The second feature comes from electrons moving within the $|z\rangle$ polarized parts, with the strongly renormalized hopping $\propto\tilde{t}_{i,i+1}$ (21) for aligned $|z\rangle$ orbitals along an almost perfect AF bond. If the AF order were perfect, the bandwidth would vanish, because no hopping would then be possible. Both the dispersive and the dispersionless structures are broadened owing to thermal fluctuations of the core spins. The superposition of these two bands yields a single peak with large intensity for $k=0$, because the bandwidth is approximately $\sim 0.5t=4J$ and therefore the both bands coincide at this point. For the same reason, the spectral weight at $k=\pi$ consists of two almost symmetric maxima. This interpretation is corroborated by the results for $\beta t=50$ (not shown), where (i) the dispersionless feature has a higher weight, because the population of $|x\rangle$ orbitals increases with increasing temperature (see Table I), and (ii) the structures in $A(k,\omega)$ are still more broadened because of the larger thermal fluctuations.

The spectrum changes rapidly when doping increases. At doping of $x=1/12$ (one hole in an $N=12$ chain) a polaronic peak is found above μ, while below μ the spectrum separates into a broad incoherent part at intermediate energies, and a low-energy peak with large intensity for low values of $k=0$ and $k=\pi/6$, being a symmetric image of the polaronic peak (not shown). As N_x decreases (Table I), the $|x\rangle$ intensity below μ drops in doped chains. At doping $x=1/6$, $|x\rangle$ electrons were found only in some samples at low temperature ($\beta t=100$). It seems that these fluctuations alone would not suffice to make the system insulating, but AF correlations are still strong here (Fig. 16) and generate a well-formed polaronic peak in the density of states for the electronic excitations (with $\omega>\mu$), separated by a pseudogap from the incoherent spectrum due to $|z\rangle$ hole excitations [Fig. 18(a)]. In this case the (localized) $|x\rangle$ excitations are predominantly electronic, leading to a distinct nondispersive peak above μ. Except for these latter excitations, the situation is here very similar to that found in the one-orbital model,[11] where FM polarons, generated by doping, were embedded into an AF background.

For the present parameters, doping $x=1/4$ (by three holes) gives an almost perfect metallic chain (occupied $|z\rangle$ orbitals) at low temperature $\beta t=100$, and the $|z\rangle$ excitations are then coherent [Fig. 18(b)]. One finds seven excitations obtained for different momenta which sum up to five distinct structures in the density of states $n(\omega)$—the two side features consist of two peaks each, representing joined intensities for $k=0$, $\pi/6$ and for $k=5\pi/6$, π, respectively. An apparent pseudogap at $\omega=\mu$ is a finite size effect and would disappear at large system sizes.

D. Jahn-Teller effect at finite temperature

We have shown above that the orbital and magnetic order are interrelated and influence each other. Therefore, as

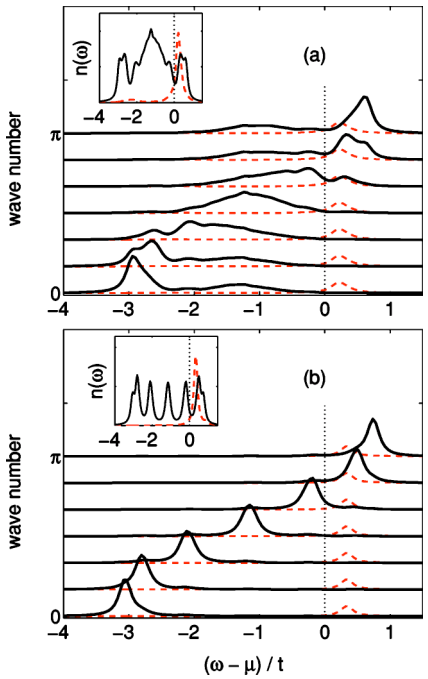

FIG. 18. (Color online) Spectral functions $A(k,\omega)$ as obtained for an $N=12$ orbital chain (20) at temperature $\beta t=100$ doped by (a) two holes and (b) three holes. Solid and dashed lines, inset and parameters as in Fig. 17.

pointed out before,[20] not only the superexchange, but also purely orbital interactions which follow from the JT effect, are of importance for the observed magnetic *A*-AF order in $LaMnO_3$. Now we will show that also in the present 1-D model the JT effect may modify the magnetic order. This is particularly transparent by considering a uniformly polarized insulating state with occupied $|z\rangle$ orbitals, coexisting with an AF order, and stabilized by weak superexchange $J'=0.02t$ (Fig. 16). If an alternating JT potential, given by Eq. (6), increases, the AF order is easily destabilized—already at $E_{\rm JT}=0.25t$ we found an almost perfect orbital staggering in the broad temperature regime at half filling [Fig. 14(c)], which induces instead the FM spin order, visible as a broad maximum in $S(k)$ centered at $k=0$ (Fig. 19). However, this maximum is less pronounced and other correlations $S(k)$ with $k>0$ are also present, unlike for $J'=E_{\rm JT}=0$, showing that the FM order induced by the JT potential is definitely much weaker.

Even for moderate JT potential $E_{\rm JT}=0.25t$, increasing doping does not change the spectral properties qualitatively, and they remain dominated by localized excitations. For doping with one hole (not shown), two localized $|x\rangle$ excitations are accompanied by three localized $|z\rangle$ excitations: the central peak corresponding to a localized hole between two $|x\rangle$ electrons, and two satellite structures, a hole excitation at energy $\omega-\mu\sim-2t$ (with large intensity for low k values), and an electron excitation at energy $\omega-\mu\sim 0.5t$, mainly contributing for large k values. These structures are similar to those found before at $T=0$ [Fig. 12(a)], but they are now broadened by thermal spin fluctuations. When doping increases, the intensity of $|x\rangle$ hole excitations decreases and moves to the Fermi energy $\omega=\mu$, while a satellite peak

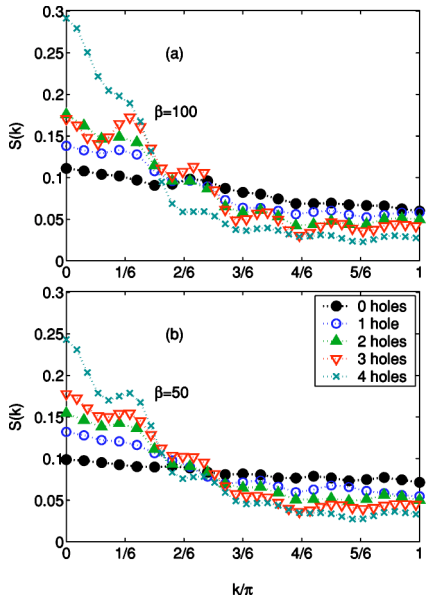

FIG. 19. (Color online) Spin structure factor $S(k)$ as in Fig. 15, but for up to four holes. Parameters: $J=0.125t$, $J'=0.02t$, $E_{\mathrm{JT}}=0.25t$.

grows for electron excitations ($\omega>\mu$), as shown for doping $x=1/4$ in Fig. 20(a). At this doping the FM correlations are enhanced by a factor ~ 1.5 with respect to the undoped case, but are still much weaker than those found before at the same doping for $E_{\mathrm{JT}}=0$ (Fig. 16), where the FM phase was metallic. This demonstrates that the intersite magnetic correlations and the energy responsible for them are weaker in insulating FM manganites than in the metallic ones at the same doping.

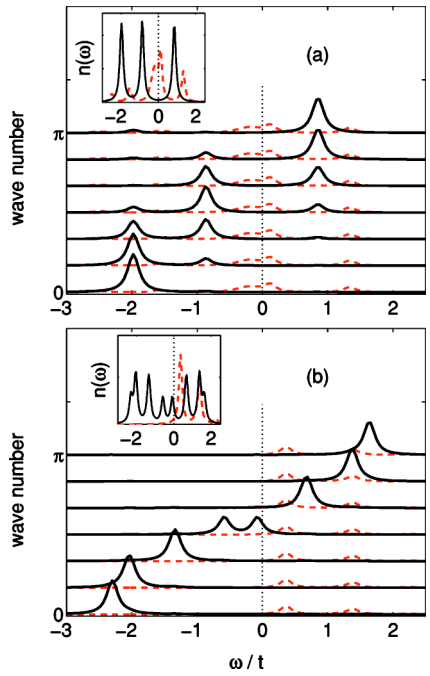

FIG. 20. (Color online) Spectral functions $A(k,\omega)$ for an $N=12$ orbital chain (20), as obtained at temperature $\beta t=100$ for (a) three holes and (b) five holes. Solid/dashed lines and inset are as in Fig. 17. Parameters: $J=0.125t$, $J'=0.02t$, $E_{\mathrm{JT}}=0.25t$.

A similar trend was indeed observed for the values of the Curie temperature T_C,[46] and one expects that also spin stiffness should be reduced by the JT coupling in CMR manganites.[47]

The transition to the metallic phase is damped by the JT distortions, and although the FM correlations increase significantly at doping $x=1/3$ (Fig. 19), the chain remains insulating. Only for as high doping as $x=5/12$, the $|x\rangle$ electrons are practically eliminated in the considered temperature range $\beta t\geqslant 50$, and a metallic behavior takes over. This metallic state gives almost free dispersion of $|z\rangle$ states in $A(k,\omega)$, while $|x\rangle$ (electron) excitations are again localized [Fig. 20(b)].

V. SUMMARY AND CONCLUSIONS

In the present study we clarify that orbital degrees of freedom are of crucial importance for the understanding of magnetic correlations in CMR manganites. First of all, for the realistic parameters of manganites the FM and AF state are nearly degenerate at half filling. In both cases the decisive term stabilizing the magnetic order originates from the e_g superexchange. Although the ground state at $T=0$ would be FM in the absence of the AF superexchange between core spins, it is easy to flip the balance of magnetic (and orbital) interactions and stabilize instead the AF order in a purely electronic model. Here we adopted the AF interaction $J'=0.02t$ between core spins in order to stabilize the AF spin order in an undoped chain (the true value of $J'\simeq 0.004t$ in $LaMnO_3$, estimated from the value of the Néel temperature of $CaMnO_3$, is smaller by a factor close to five[20]), and to demonstrate a gradual crossover from an AF insulator to a FM metal under increasing doping. In this regime of parameters the present 1-D chain stands for the AF order along the c axis in the A-AF phase realized in $LaMnO_3$.

We have shown that *even in the 1-D model* the magnetic interactions are internally frustrated, with competing FM and AF terms in the superexchange. A delicate balance between these terms is easily disturbed by the JT potential originating from the lattice. This allows one to investigate within the same framework both types of magnetic order which coexist in the A-AF phase of undoped manganites. On one hand, if the oxygen distortion have almost no influence, or if a uniform polarization in $|z\rangle$ orbitals would be induced by them, the AF spin order, found along the c axis in the A-AF phase of $LaMnO_3$, would be supported. On the other hand, if the oxygen distortions are alternating, they induce alternating orbital order, as it happens in (a,b) planes of $LaMnO_3$, and the FM terms are selected from the e_g superexchange. Note, however, that the FM correlations are weakly reduced from their values found in the absence of the JT interations ($J'=0$ and $E_{\mathrm{JT}}=0$), demonstrating that the FM interactions do not depend *explicitly* on the JT terms, but are only induced by a given type of orbital order. In this way the JT coupling to the lattice helps to remove the frustration of magnetic interactions in CMR manganites.

The evolution of spin correlations for increasing doping showed that indeed two mechanisms are responsible for ferromagnetism: when the weakly doped 1-D chain is insulat-

ing, the FM interactions are induced both by the *superexchange* terms following from the high-spin excited states, and by the local double exchange within polaronic states around single holes trapped in the insulating phase. The *double exchange* interaction is much stronger than the superexchange, and it fully takes over and operates in the metallic phase at higher doping. The difference between these two mechanisms is reflected by a fast increase of FM correlations at the insulator-metal transition which was investigated both within a purely electronic model, and including the JT potential induced by the lattice.

It is quite remarkable that *orbital polarons* found in the present model with orbital degeneracy in the regime of AF spin correlations resemble FM polarons which occur in the Kondo model.[11] This provides some support to a simplified picture of a nondegenerate conduction band which is able to capture the essential physics when the orbitals are polarized, and the orbital degrees of freedom are quenched and do not contribute in any significant way. A conservative point of view, based on a double exchange mechanism, is that the FM polarons compete with the AF order and cause a transition to the metallic FM phase. Yet, this is not the only possibility—we have shown that the FM phase at low doping could be insulating due to immobile orbital polarons, which allow us to understand why this phase could be FM and insulating at the same time. Such polarons are expected to play an essential role in the insulator-metal transition within the FM phase in manganites.

We believe that many qualitative features found in the present 1-D study are generic for the interplay between orbital and magnetic order in CMR manganites. Work is in progress on higher dimensional systems. Among others, an interesting question is to what extent the orbital order is modified when two e_g orbitals start to fluctuate more strongly in either 2-D or 3-D systems, both due to quantum effects and due to increasing doping.

ACKNOWLEDGMENTS

We thank E. Arrigoni and A. Prüll for valuable discussions. This work has been supported by the Austrian Science Fund (FWF), Project No. P15834-PHY. A. M. Oleś would like to acknowledge the kind hospitality of the Institute of Theoretical and Computational Physics, Graz University of Technology, and support by the Polish State Committee of Scientific Research (KBN) under Project No. 1 P03B 068 26.

[1] E. Dagotto, *Nanoscale Phase Separation and Colossal Magnetoresistance* (Springer-Verlag, Heidelberg, 2003); E. Dagotto, T. Hotta, and A. Moreo, Phys. Rep. **344**, 1 (2001).

[2] S. Jin, T. H. Tiefel, M. McCormack, R. A. Fastnacht, R. Ramesh, and L. H. Chen, Science **264**, 413 (1994); P. Schiffer, A. P. Ramirez, W. Bao, and S.-W. Cheong, Phys. Rev. Lett. **75**, 3336 (1995); A. Urushibara, Y. Moritomo, T. Arima, A. Asamitsu, G. Kido, and Y. Tokura, Phys. Rev. B **51**, 14103 (1995).

[3] C. Zener, Phys. Rev. **82**, 403 (1951).

[4] T. V. Ramakrishnan, H. R. Krishnamurthy, S. R. Hassan, and G. Venketeswara Pai, Phys. Rev. Lett. **92**, 157203 (2004).

[5] S. Yunoki, J. Hu, A. L. Malvezzi, A. Moreo, N. Furukawa, and E. Dagotto, Phys. Rev. Lett. **80**, 845 (1998); E. Dagotto, S. Yunoki, A. L. Malvezzi, A. Moreo, J. Hu, S. Capponi, D. Poilblanc, and N. Furukawa, Phys. Rev. B **58**, 6414 (1998).

[6] N. Furukawa, in *Physics of Manganites*, edited by T. A. Kaplan and S. D. Mahanti (Kluwer Academic, New York, 1999).

[7] D. M. Edwards, A. C. Green, and K. Kubo, J. Phys.: Condens. Matter **11**, 2791 (1999); A. C. Green and D. M. Edwards, *ibid.* **11**, 10511 (1999); M. Hohenadler and D. M. Edwards, *ibid.* **14**, 2547 (2002).

[8] H. Aliaga, B. Normand, K. Hallberg, M. Avignon, and B. Alascio, Phys. Rev. B **64**, 024422 (2001).

[9] W. Nolting, G. G. Reddy, A. Ramakanth, and D. Meyer, Phys. Rev. B **64**, 155109 (2001); C. Santos and W. Nolting, *ibid.* **66**, 019901 (2002).

[10] W. Koller, A. Prüll, H. G. Evertz, and W. von der Linden, Phys. Rev. B **66**, 144425 (2002); **67**, 104432 (2003).

[11] W. Koller, A. Prüll, H. G. Evertz, and W. von der Linden, Phys. Rev. B **67**, 174418 (2003).

[12] P. Horsch, J. Jaklič, and F. Mack, Phys. Rev. B **59**, 6217 (1999); J. Bała, P. Horsch, and F. Mack, *ibid.* **69**, 094415 (2004).

[13] J. van den Brink and D. I. Khomskii, Phys. Rev. Lett. **82**, 1016 (1999); K. Held and D. Vollhardt, *ibid.* **84**, 5168 (2000); M. S. Laad, L. Craco, and E. Müller-Hartmann, Phys. Rev. B **63**, 214419 (2001).

[14] A. M. Oleś and L. F. Feiner, Phys. Rev. B **65**, 052414 (2002).

[15] K. I. Kugel and D. I. Khomskii, Usp. Fiz. Nauk **136**, 621 (1982) [Sov. Phys. Usp. **25**, 231 (1982)].

[16] Y. Tokura and N. Nagaosa, Science **288**, 462 (2000); A. M. Oleś, Phys. Status Solidi B **236**, 281 (2003).

[17] L. F. Feiner, A. M. Oleś, and J. Zaanen, Phys. Rev. Lett. **78**, 2799 (1997); A. M. Oleś, L. F. Feiner, and J. Zaanen, Phys. Rev. B **61**, 6257 (2000).

[18] R. Shiina, T. Nishitani, and H. Shiba, J. Phys. Soc. Jpn. **66**, 3159 (1997).

[19] S. Maezono, S. Ishihara, and N. Nagaosa, Phys. Rev. B **57**, R13 993 (1998); **58**, 11583 (1998).

[20] L. F. Feiner and A. M. Oleś, Phys. Rev. B **59**, 3295 (1999).

[21] S. Okamoto, S. Ishihara, and S. Maekawa, Phys. Rev. B **65**, 144403 (2002).

[22] Y. Murakami, J. P. Hill, D. Gibbs, M. Blume, I. Koyama, M. Tanaka, H. Kawata, T. Arima, Y. Tokura, K. Hirota, and Y. Endoh, Phys. Rev. Lett. **81**, 582 (1998); J. Rodríguez-Carvajal, M. Hennion, F. Moussa, A. H. Moudden, L. Pinsard, and A. Revcolevschi, Phys. Rev. B **57**, R3189 (1998).

[23] J. van den Brink, P. Horsch, F. Mack, and A. M. Oleś, Phys. Rev. B **59**, 6795 (1999).

[24] G. Biotteau, M. Hennion, F. Moussa, J. Rodríguez-Carvajal, L. Pinsard, A. Revcolevschi, Y. M. Mukovskii, and D. Shulyatev, Phys. Rev. B **64**, 104421 (2001); F. Moussa, M. Hennion, F. Wang, P. Kober, J. Rodríguez-Carvajal, P. Reutler, L. Pinsard, and A. Revcolevschi, *ibid.* **67**, 214430 (2003).

[25] Y. Endoh, K. Hirota, S. Ishihara, S. Okamoto, Y. Murakami, A.

Nishizawa, T. Fukuda, H. Kimura, H. Nojiri, K. Kaneko, and S. Maekawa, Phys. Rev. Lett. **82**, 4328 (1999).
[26] A. Weiße, J. Loos, and H. Fehske, Phys. Rev. B **64**, 054406 (2001); **68**, 024402 (2003).
[27] J. van den Brink, P. Horsch, and A. M. Oleś, Phys. Rev. Lett. **85**, 5174 (2000); W.-G. Yin, H.-Q. Lin, and C.-D. Gong, *ibid.* **87**, 047204 (2001).
[28] J. Bała, A. M. Oleś, and P. Horsch, Phys. Rev. B **65**, 134420 (2002).
[29] A. Ramšak and P. Horsch, Phys. Rev. B **48**, 10559 (1993); **57**, 4308 (1998).
[30] J. Bonča, P. Prelovšek, I. Sega, H. Q. Lin, and D. K. Campbell, Phys. Rev. Lett. **69**, 526 (1992).
[31] P. Wróbel and R. Eder, Phys. Rev. B **54**, 15882 (1996).
[32] P. Benedetti and R. Zeyher, Phys. Rev. B **59**, 9923 (1999).
[33] T. Hotta, A. L. Malvezzi, and E. Dagotto, Phys. Rev. B **62**, 9432 (2000).
[34] R. Kilian and G. Khaliullin, Phys. Rev. B **60**, 13458 (1999).
[35] K. A. Chao, J. Spałek, and A. M. Oleś, J. Phys. C **10**, L271 (1977); Phys. Rev. B **18**, 3453 (1978).
[36] The FM ground state is found for realistic parameters of manganites. However, a somewhat smaller Hund's exchange J_H, or large AF superexchange J' between t_{2g} core spins, would give instead an AF ground state with uniformly polarized $|z\rangle$ orbitals at $n=1$.
[37] T. Hotta, Phys. Rev. B **67**, 104428 (2003).
[38] A. Millis, Phys. Rev. B **53**, 8434 (1996).
[39] J. Bała and A. M. Oleś, Phys. Rev. B **62**, R6085 (2000).
[40] G. Martínez and P. Horsch, Phys. Rev. B **44**, 317 (1991).
[41] M. G. Zacher, E. Arrigoni, W. Hanke, and J. R. Schrieffer, Phys. Rev. B **57**, 6370 (1998).
[42] D. Sénéchal, D. Perez, and M. Pioro-Ladrière, Phys. Rev. Lett. **84**, 522 (2000).
[43] M. Aichhorn, M. Daghofer, H. G. Evertz, and W. von der Linden, Phys. Rev. B **67**, 161103(R) (2003).
[44] J. Zaanen, A. T. Paxton, O. Jepsen, and O. K. Andersen, Phys. Rev. Lett. **60**, 2685 (1988).
[45] Y. Endoh and K. Hirota, J. Phys. Soc. Jpn. **66**, 2264 (1997).
[46] J. A. Fernandez-Baca, P. Dai, H. Y. Hwang, C. Kloc, and S-W. Cheong, Phys. Rev. Lett. **80**, 4012 (1998).
[47] S. Maezono and N. Nagaosa, Phys. Rev. B **67**, 064413 (2003).